Multiple wavelength DFB laser arrays with high coupling coefficient and precise channel spacing

SONG TANG,[1] LIANPING HOU,[1] XIANGFEI CHEN,[2] JOHN H. MARSH[1,*]

[1]*School of Engineering, University of Glasgow, Glasgow G12 8QQ, U.K.*
[2] *College of Engineering and Applied Sciences, Nanjing University, Nanjing 210093, China*
**Corresponding author: John.Marsh@glasgow.ac.uk*

Received XX Month XXXX; revised XX Month, XXXX; accepted XX Month XXXX; posted XX Month XXXX (Doc. ID XXXXX); published XX Month XXXX

Special designs of sampled Bragg gratings have been used to fabricate distributed feedback semiconductor laser arrays with very precise wavelength spacing and strong coupling coefficients. By dividing one sampling period into two equal sections, each with a grating but with a π-phase shift between the sections, the ±1st-order channels are enhanced while eliminating the 0th-order reflection. By using multiple phase-shifted sections, only the −1st-order channel is enhanced. Using a single electron beam lithography step and two π-phase shifted sections, we have fabricated an eight-channel laser array with channel spacing of 100 GHz.

OCIS codes: *(140.3490) Lasers, distributed-feedback; (130.5990) Semiconductors; (230.5590) Quantum-well, -wire and -dot devices; (050.5080) Phase shift.*

http://dx.doi.org/10.1364/OL.99.099999

Distributed feedback (DFB) semiconductor laser arrays are of substantial interest in wavelength division multiplexing networks for higher data capacity, especially for low-cost applications in data centers and access networks [1, 2]. The lasing wavelength of a DFB laser diode depends on the effective refractive index of the waveguide and the corrugation pitch of the grating. To obtain different lasing wavelengths, we usually choose to change the corrugation pitch, often defined by electron beam lithography (EBL), and in this way a wide range of wavelengths can be accessed [3]. However, the pattern unit of the EBL machine limits the resolution at which the corrugation pitch can be written; for example, to define an array with spacing of 100 GHz, the resolution needs to be about 0.125 nm, which is beyond the typical resolution limit of 0.5 nm of EBL machines.

There is therefore a need to improve the resolution for grating definition beyond the standard resolution of EBL systems. One such method is weighted-dose allocation variable-pitch EB-lithography, but the associated algorithm makes the technique complex and ill-suited to volume manufacture [4]. Recently the reconstruction-equivalent-chirp (REC) technique has been demonstrated to give precise wavelength control in a simple way based on sampled Bragg gratings (SBGs) [5, 6]. However, the effective coupling coefficient, κ, of the grating in the DFB laser is reduced substantially compared to that of a continuous uniform grating, which adversely affects the single longitudinal mode (SLM) performance of the laser. To increase the coupling coefficient, sampled Bragg grating structures with multiple phase-shifted sections have been proposed and demonstrated in fiber lasers [7]. In these structures, the strength of the ±1st-order reflections can be enhanced selectively, while suppressing the 0th-order reflection.

Here, we have successfully combined phase-shifted SBGs with the REC technique to fabricate DFB laser arrays using a single EBL step. We have studied a number of phase-shifted designs and demonstrated that the effective coupling coefficients in single-mode diode lasers increase as a result. By changing the sampling periods and using 2-section SBG designs, we have fabricated an eight-channel laser array operating around 1550 nm with channel spacing of 100 GHz (equivalent to ~0.8 nm) and increased coupling coefficient.

The principle of introducing phase-shifted sections into SBGs is illustrated in Fig. 1, where various designs are shown. In all cases discussed here, the working channels use the ±1st-order reflections. Figure 1(a) shows the design of a conventional SBG (C-SBG), which is designed with a duty cycle of 0.5 to obtain the largest effective coupling coefficient for the ±1st-order channels. Previously, this design of SBG was used to fabricate a large (60-element) array of DFB lasers using the REC technique [5]. However, the κ associated with the ±1st -order channels is only $1/\pi$ (~ 0.32) times of that of uniform gratings. Such a large reduction in κ is not desirable; either the cavity length of the laser (L) has to be increased to maintain an optimum κL product at the expense of an increase in threshold current, or κL is reduced which will affect the stability of SLM operation. Furthermore, although in this structure the 0th-order reflection strength is reduced to half of that of a uniform grating (no sampling), it remains the strongest reflection and its presence may affect the operation of the working channels.

Designs of SBGs that incorporate phase shifted sections can overcome these defects, by simultaneously enhancing the effective κ of the ±1st-order channels and eliminating the 0th-order reflection. The theoretical analysis and simulation results have been presented previously [7]. Figure 1(b) illustrates an SBG with two phase-shifted

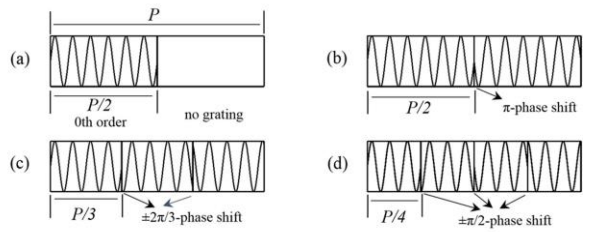

Fig. 1. Grating structures of (a) C-SBG (b) 2PS-SBG (c) 3PS-SBG (d) 4PS-SBG, P is the sampling period.

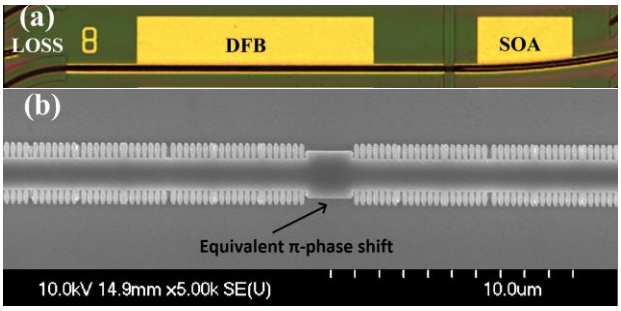

Fig. 2. (a) Micrograph of fabricated device, and (b) SEM image of a 2PS-SBG with equivalent π-phase shift.

sections in a single sampling period (2PS-SBG), in which a π-phase shifted 0th-order grating fills a half of the sampling period where the grating would be absent in a C-SBG. In a 2PS-SBG structure, the 0th-order reflection disappears and the effective κ of the ±1st-order channels is doubled compared to the C-SBG, with a value of $2/\pi$ (~0.64) times that of a uniform grating. We can further divide the sampling period into more sections to obtain progressively higher effective κ. If we divide one sampling period P into m equal sections (m>2), with length of P/m in every section, the phase shift between adjacent sections can be set as $\pm 2\pi/m$. When the phase shift is $-2\pi/m$, simulation shows the κ of the −1st-order channel will be enhanced, with both the 0th-order and 1st-order channels suppressed, and vice versa. Figure 1(c) shows an SBG with three phase-shifted sections (3PS-SBG) and Fig. 1(d) illustrates an SBG with four phase-shifted sections (4PS-SBG), the effective κ of which are calculated to be about 0.83 and 0.90 times that of a uniform grating. To obtain single-mode lasing, it is straightforward to introduce equivalent π-phase shifts ('quarter wavelength step' design) into the sampled waveguide. By applying the REC principles, DFB diode lasers with different lasing wavelengths can be realized with high precision by changing only the sampling period.

We report the application of these design concepts to DFB lasers based on ridge waveguides with sidewall gratings. Ridge waveguides offer a versatile route to device integration that eliminates the oxidation and contamination problems associated with regrowth. Compared to buried heterostructure devices, the threshold current of ridge waveguides is higher because of the wider waveguide and current spreading. However, ridge waveguide devices generally deliver higher optical powers, an important consideration for transceivers in passive optical networks (PONs). While the grating coupling coefficient of

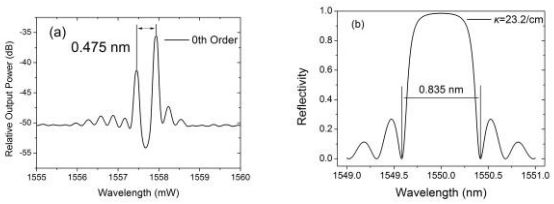

Fig. 3. (a) Optical spectrum of a laser diode just below threshold (50 mA) with uniform 0th-order grating, and (b) the simulated reflection spectrum of a passive waveguide of the corresponding uniform grating.

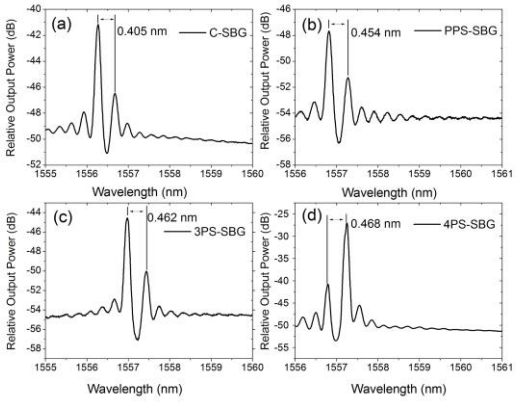

Fig. 4. Optical spectra measured just below threshold (50 mA) of (a) C-SBG, (b) 2PS-SBG, (c) 3PS-SBG and (d) 4PS-SBG.

overgrown structures can be made larger than that of sidewall gratings, higher power or narrow linewidth applications demand a longer cavity, and so ridge waveguide sidewall gratings have many practical applications.

The devices were fabricated using similar process steps to reference [8]. Figure 2(a) shows an optical micrograph of one of the fabricated laser diodes. The cavity length L of the DFB section is 1200 μm and the SOA has a length of 300 μm, separated by an isolation region of 20 μm. The SOA has a curved waveguide with radius of 1724.1 μm making an angle of 10° at the output facet. To avoid back reflections from the other side of the laser diode, a waveguide, of length 125 μm with a radius of 233.3 μm and an angle of 32° at the facet, absorbs the light. The curved waveguides minimize back reflections from the facets, so the lasing wavelength only depends on the gratings in the DFB section. Figure 2(b) shows a scanning electron microscope (SEM) image of a 2PS-SBG with equivalent π-phase shift in the center of the DFB laser cavity.

Firstly, a laser diode with a uniform 0th-order grating with a period of 243 nm without sampling was fabricated as a reference. We measured the optical spectrum with the injection currents of the DFB section and the SOA set just below threshold (50 mA) and at 5 mA respectively. The stop band between the two main modes is 0.475 nm, as shown in Fig. 3(a), from which κ is calculated to be 23.2 cm^{-1}. The corresponding reflection spectrum of a passive waveguide with the same uniform grating parameters was simulated using a simple transfer matrix method, and, as shown in Fig. 3(b), the stop band is 0.835 nm. It is well known that the measured stop band of a DFB grating in the presence of gain is

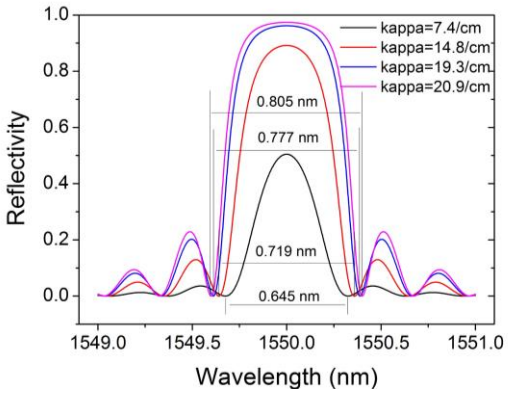

Fig. 5. Simulated reflection spectra of passive waveguides with different values of κ (smallest κ having narrowest stopband).

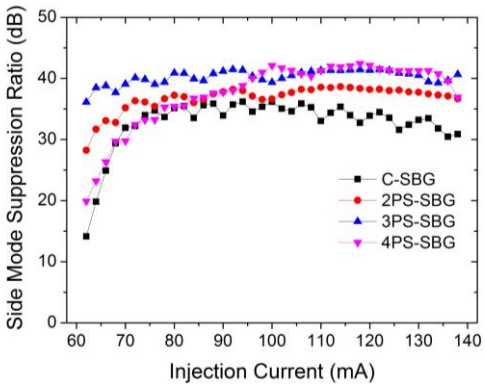

Fig. 6. SMSRs of the lasers as a function of laser injection current with the injection current of the SOA set at 20 mA.

Table 1. Properties of modelled and measured gratings

Grating types	C-SBG	2PS-SBG	3PS-SBG	4PS-SBG	Uniform 0th-order grating
Measured band gap / nm	0.405	0.454	0.462	0.468	0.475
Uniform grating Equivalent κ / cm^{-1}	7.4	14.8	19.3	20.9	23.2
Uniform grating Passive stop band / nm	0.645	0.719	0.777	0.805	0.835
Ratio of {measured /passive stop band}	0.63	0.63	0.59	0.58	0.57

significantly smaller than that of the equivalent passive waveguide [9], which accounts for the difference.

We also fabricated SBG lasers with no quarter wavelength steps corresponding to the four designs presented in Fig. 1. To obtain the same operating wavelength as the reference laser, the 0th-order grating period was set at 260 nm and the sampling period was 3.712 μm. Here, we choose the −1st-order channel as the working channel, so the appropriate phase shifts for the 3PS-SBG and 4PS-SBG designs are $-2\pi/3$ and $-2\pi/4$ respectively. With the same injection currents as for the reference laser, we measured the optical spectra of these structures just below threshold, as shown in Fig. 4.

The measured stop bands of the C-SBG, 2PS-SBG, 3PS-SBG and 4PS-SBG lasers are 0.405 nm, 0.454 nm, 0.462 nm and 0.468 nm respectively. Since the theoretical ratios of the effective κ of the −1st-order channels to that of the 0th-order channel are about 0.32, 0.64, 0.83 and 0.90 respectively, the effective κ of -1st-order channels are estimate as 7.4 cm^{-1}, 14.8 cm^{-1}, 19.3 cm^{-1} and 20.9 cm^{-1} for C-SBG, 2PS-SBG, 3PS-SBG and 4PS-SBG respectively. The reflection spectra of passive waveguides have been simulated based on these estimate values of effective κ, shown in Fig. 5. From the simulation, the corresponding stop bands are measured to be 0.645 nm, 0.719 nm, 0.777 nm and 0.805 nm. All these data are summarized in Table 1 and where we also present the calculated ratios of the stop bands of active waveguides and stop bands of passive waveguides. Since the ratios are almost constant (0.6 ± 0.03), we conclude the effective coupling coefficients are approximately the same as the theoretical values. We conclude the reflection strengths of the −1st-order channels are indeed enhanced as expected.

The side mode suppression ratios (SMSRs) of the lasers are shown in Fig. 6 as a function of drive current, with the injection current of the SOA set at 20 mA. Stable SLM operation is observed when the DFB injection current is more than 70 mA. We also observe an increase in the SMSR with the number of phase-shifted sections in one sampling period, reflecting the increase in the effective coupling coefficient. Figure 7 shows the optical spectra from the various SBG DFB lasers when the injection currents of the DFB and SOA sections were set at 100 mA and 20 mA respectively. The Fabry-Pérot modes are barely visible in the spectra, implying that the facet reflection and the reflection from the shallow etched isolation slot between the DFB and SOA are negligible.

Finally, we have fabricated and characterized an eight-wavelength laser array using a 2PS-SBG design. The 0th-order channel was chosen to be 250 nm, and the sampling period varied from 7.979 μm to 9.206 μm, to give a channel spacing of 100 GHz, corresponding to ~0.8 nm at 1550 nm. To ensure SLM operation of the DFB lasers, the central section contains the equivalent quarter wavelength phase shift, shown in Fig. 2(b). The laser array was measured with the injection currents of the DFB and SOA sections set at 100 mA and 20 mA respectively. The lasing spectra are shown in Fig. 8(a). The difference in peak power between the lasers is not significant, and reflects variations in coupling the light from the SOAs into the single mode fiber used to feed the optical spectrum

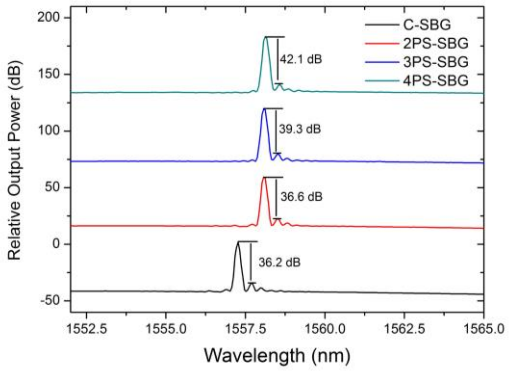

Fig. 7. Optical spectra of various SBGs at 100 mA.

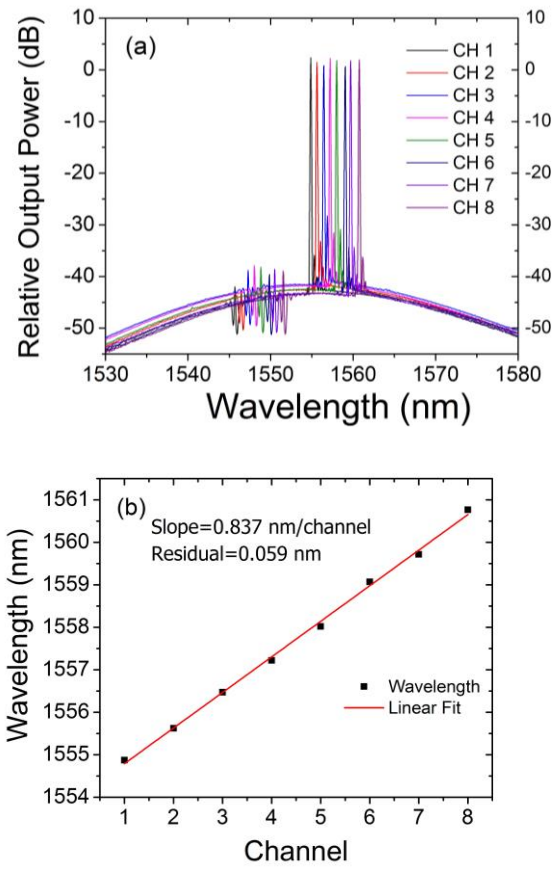

Fig. 8. (a) Optical spectra of the laser array at 100 mA (channels 1 to 8, left to right), (b) linear fitting of the wavelengths.

analyzer. By linear fitting of the wavelengths, we obtain a slope of 0.837 nm per channel (104 GHz), with a residual of 0.059 nm (Fig. 8(b)). These results demonstrate the excellent wavelength precision that can be achieved with this technique.

Figure 9 shows the light-current-voltage (*LIV*) curves of the lasers. The devices were measured with a drive current of 40 mA applied to the appropriate SOA. Given each of the *L-I* characteristics reflects the performance of a laser/SOA combination, the uniformity of optical output power is acceptable. The lasers reported here have been designed with relatively long cavities (1200 μm) to deliver light with high power required by PONs – Fig. 9 shows almost 10 dBm with the SOA driven at 40 mA. Electro-absorption modulators will be integrated within future iterations of the DFB laser array to make an optical transmitter, suitable for use in PONs and data centers.

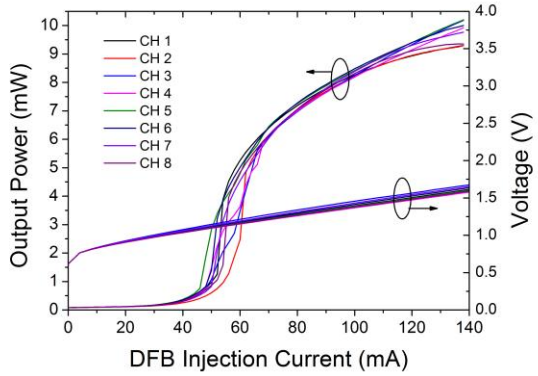

Fig. 9. *LIV* characteristics of the fabricated eight-wavelength laser array based on a 2PS-SBG design. The SOA drive current was 40 mA.

In conclusion, SBGs with multiple phase-shifted sections have been successfully applied to DFB semiconductor lasers and laser arrays. By comparing the stop bands of active waveguides with the stop bands of passive waveguides, the expected increase of effective coupling coefficients with number of phase sections has been demonstrated. By combining phase-shifted sections with the REC technique (including an equivalent π-phase shift), single-mode lasing of DFB diode lasers was also realized successfully. For 4PS-SBG devices, the effective coupling coefficient was close to that of uniform gratings (estimated to be 21 cm^{-1} compared to 23 cm^{-1}). By simply changing the sampling periods, an eight-wavelength laser array with channel spacing of 100 GHz was fabricated. These results demonstrate the advantages of our approach over conventional methods of fabricating DFB lasers using EBL. The fabrication flow is straightforward, requiring only a single EBL step and no regrowth. SBGs with multiple phase-shifted sections are a powerful approach for breaking through the limitations imposed by the resolution of EBL machines. The approach can be applied readily to the volume manufacture of DFB semiconductor lasers and laser arrays.

Acknowledgment. We would like to acknowledge the staff of the James Watt Nanofabrication Centre at the University of Glasgow for their assistance in fabricating the devices.

References

1. L. Schares, Y. H. Lee, D. Kuchta, U. Koren, and L. Ketelsen, in Optical Fiber Communication Conference (OFC), OSA Technical Digest (Optical Society of America, 2014), paper Th1C.3.
2. O. K. Kwon, Y. A. Leem, Y. T. Han, C. W. Lee, K. S. Kim, and S. H. Oh, Opt. Express 22, 9073 (2014).
3. T. Kurobe, T. Kimoto, K. Muranushi, Y. Nakagawa, H. Nasu, S. Yoshimi, M. Oike, H. Kambayashi, T. Mukaihara, T. Nomura, and A. Kasukawa, Electron. Lett. 39, 1125 (2003).
4. Y. Muroya, T. Nakamura, H. Yamada, and T. Torikai, IEEE Photon. Technol. Lett. 9, 288 (1997).
5. Y. Shi, S. Li, X. Chen, L. Li, J. Li, T. Zhang, J. Zheng, Y. Zhang, S. Tang, and L. Hou, Scientific Reports 4, 7377 (2014).
6. Y. Shi, X. Chen, Y. Zhou, S. Li, L. Lu, R. Liu, and Y. Feng, Opt. Lett. 37, 3315 (2012).
7. J. Li, Y. Cheng, Z. Yin, L. Jia, X. Chen, S. Liu, S. Li, and Y. Lu, IEEE Photon. Technol. Lett. 21, 1639 (2009).
8. L. Hou, M. Haji, J. Akbar, J. H. Marsh, and A. C. Bryce, IEEE J. Quantum Electron. 48, 137-143.
9. T. Ikegami, "Longitudinal mode control in laser diodes," in Optoelectronic Technology and Lightwave Communications Systems, C. Lin, ed. (Van Nostrand Reinhold, 1989), p. 264.

References

1. L. Schares, Y. H. Lee, D. Kuchta, U. Koren, and L. Ketelsen, "An 8-Wavelength Laser Array with High Back Reflection Tolerance for High-Speed Silicon Photonic Transmitters," in *Optical Fiber Communication Conference (OFC),* OSA Technical Digest (Optical Society of America, 2014), paper Th1C.3.
2. O. K. Kwon, Y. A. Leem, Y. T. Han, C. W. Lee, K. S. Kim, and S. H. Oh, "A 10× 10 Gb/s DFB laser diode array fabricated using a SAG technique," Opt. Express **22**, 9073-9080 (2014).
3. T. Kurobe, T. Kimoto, K. Muranushi, Y. Nakagawa, H. Nasu, S. Yoshimi, M. Oike, H. Kambayashi, T. Mukaihara, T. Nomura, and A. Kasukawa, "High fibre coupled output power 37 nm tunable laser module using matrix DFB laser," Electron. Lett. **39**, 1125-1126 (2003).
4. Y. Muroya, T. Nakamura, H. Yamada, and T. Torikai, "Precise wavelength control for DFB laser diodes by novel corrugation delineation method," IEEE Photon. Technol. Lett. **9**, 288-290 (1997).
5. Y. Shi, S. Li, X. Chen, L. Li, J. Li, T. Zhang, J. Zheng, Y. Zhang, S. Tang, and L. Hou, "High channel count and high precision channel spacing multi-wavelength laser array for future PICs," *Scientific reports* **4**, 7377 (2014).
6. Y. Shi, X. Chen, Y. Zhou, S. Li, L. Lu, R. Liu, and Y. Feng, "Experimental demonstration of eight-wavelength distributed feedback semiconductor laser array using equivalent phase shift," Opt. Lett. **37**, 3315-3317 (2012).
7. J. Li, Y. Cheng, Z. Yin, L. Jia, X. Chen, S. Liu, S. Li, and Y. Lu, "A multiexposure technology for sampled Bragg gratings and its applications in dual-wavelength lasing generation and OCDMA en/decoding," IEEE Photon. Technol. Lett. **21**, 1639-1641 (2009).
8. L. Hou, M. Haji, J. Akbar, J. H. Marsh, and A. C. Bryce, "AlGaInAs/InP monolithically integrated DFB laser array," IEEE J. Quantum Electron. **48**, 137-143 (2012).
9. T. Ikegami, "Longitudinal mode control in laser diodes," in *Optoelectronic Technology and Lightwave Communications Systems*, C. Lin, ed. (Van Nostrand Reinhold, 1989), pp. 264–298.